

A NOVEL NUMERICAL MANNER FOR NON-LINEAR COUPLED VARIABLE ORDER REACTION-DIFFUSION EQUATION

by

Mohd KASHIF^a, Prashant PANDEY^a, and Hossein JAFARI^{b,c*}

^a Department of Mathematical Sciences Indian Institute of Technology (BHU), Varanasi, India

^b Department of Mathematical Sciences University of South Africa, Pretoria, South Africa

^c Department of Medical Research, China Medical University Hospital,
China Medical University, Taichung, Taiwan

Original scientific paper

<https://doi.org/10.2298/TSCI23S1353K>

In this work, an efficient variable order Bernstein collocation technique, which is based on Bernstein polynomials, is applied to a non-linear coupled system of variable order reaction-diffusion equations with given initial and boundary conditions. The operational matrix of Bernstein polynomials is derived for variable order derivatives w.r.t. time and space. The Bernstein operational matrix and collocation technique are applied to the concerned non-linear physical model to achieve a system of non-linear algebraic equations, which are further solved by using Newton method. A few examples are presented to demonstrate the accuracy and stability of the scheme by comparing L_2 and L_∞ norm errors between the obtained numerical solutions and existing solutions. The important feature of this article is the graphical exhibitions of the effects of variable order derivatives on the solutions of the considered non-linear coupled reaction-diffusion equation for different particular cases.

Key words: *variable order derivatives, diffusion equation, Bernstein polynomials, convergence analysis, error bounds*

Introduction

Abel and Liouville have developed the fractional calculus theory. The fractional order derivative is an extended form of integer order derivative, and the variable order (VO) derivative is an extension of fractional order derivative. Nowadays, VO PDE have been widely used in numerous fields of science. An extensive explanation of fractional calculus can be found from the literature, viz., [1-4]. Young scientists, applied mathematicians, engineers, and researchers may find a broad applications of fractional calculus in chemistry, biology, medical, image processing, and mathematical physics, etc.

The integer order differentiation is being used to characterize short term memory systems, and to extend the applications of the derivative to long term systems the fractional order derivative is being used. Moreover, to characterize the variable memory systems, the VO derivative is used. Thus the VO differential has many applications to model several physical and biological phenomena more accurately.

* Corresponding author, e-mail: jafari.usern@gmail.com

The wide applications of fractional derivatives drag the focus of mathematicians to find the numerical solutions and exact solutions of the mathematical models of numerous non-linear biological and physical processes. The exact solutions of many PDE of fractional order do not exist or cannot be found easily, so numerous numerical techniques have been invented to find their approximate solutions [5-9]. The presence of non-linear VO PDE is very important in the mathematical structure of several complex physical models.

Many definitions and properties of VO integration and differentiation can be found from literature survey. It becomes a fascinating notion in fractional calculus when we extend the concept of fractional constant order derivative to time and space dependent fractional derivative. This novel concept of fractional calculus can be used in several characteristics of mechanics, control and signal processing, mathematical physics, *etc.* [10-12]. Finding the numerical solutions of PDE with VO derivatives are a little more complicated than fractional constant order derivatives due to the VO fractional operators having complex kernels for variable powers. In Fu *et al.* [13], a finite difference technique based on the radial basis function is utilized for solving constant and VO fractional diffusion equations. Chen *et al.* [14] have proposed a numerical technique based on the implicit numerical method to solve the multi-term space-time VO fractional advection-diffusion model to describe the underlying transport dynamics. A finite difference scheme has been presented in [15] for finding the numerical solution of VO fractional differential equations along with stability and convergence analyses of the scheme. In addition, many numerical schemes are available in the literature for finding the numerical solution of VO fractional differentiation viz., spectral collocation technique, discretization technique, cubic spline technique, finite difference method, integro quadratic spline interpolations techniques, B-linear spline technique, *etc.*

The system of coupled PDE in porous media describes the interaction and diffusion of two solute species. The dealing of mathematical models of such physical phenomena is a challenging task. Several systems of coupled PDE have been discussed in constant fractional order systems viz., KdV-Burgers' equation, Boussinesq-Whitham-Broer-Kaup equation, Burgers' equation, Klein-Gordon-Zakharov equation, *etc.* These systems have a wide range of applications in many complex physical processes like plasma physics, fluid mechanics, non-linear wave theory, non-linear optics, gas dynamics, non-linear acoustics and shallow water waves, *etc.*

In this scientific research our main aim is to study a special group of non-linear coupled system of variable order reaction-diffusion equation. The main motivation behind the concerned coupled PDE is a vast applications of the model in fluid mechanics, non-linear optics and non-linear wave theory, gas dynamics, non-linear acoustics, and shallow water waves, *etc.* Many well-known systems of coupled PDE are particular cases of the concerned model. Our considered variable order coupled system of non-linear PDE is given:

$$\begin{aligned} \frac{\partial^{\mu_1(x,t)} \zeta(x,t)}{\partial t^{\mu_1(x,t)}} + p_1 \frac{\partial^{p_2} \zeta(x,t)}{\partial x^{p_2}} + p_3 \frac{\partial^{p_4} \xi(x,t)}{\partial x^{p_4}} + p_5 \zeta(x,t) \frac{\partial \zeta(x,t)}{\partial x} + p_6 \frac{\partial(\zeta(x,t)\xi(x,t))}{\partial x} &= h_1(x,t) \\ \frac{\partial^{\mu_2(x,t)} \xi(x,t)}{\partial t^{\mu_2(x,t)}} + p_1' \frac{\partial^{p_2'} \zeta(x,t)}{\partial x^{p_2'}} + p_3' \frac{\partial^{p_4'} \xi(x,t)}{\partial x^{p_4'}} + p_5' \xi(x,t) \frac{\partial \xi(x,t)}{\partial x} + p_6' \frac{\partial(\zeta(x,t)\xi(x,t))}{\partial x} &= h_2(x,t) \end{aligned} \quad (1)$$

under the initial and boundary conditions:

$$\begin{aligned} \zeta(x,0) = \lambda_1(x), \quad \zeta(0,t) = \lambda_2(t), \quad \zeta(1,t) = \lambda_3(t) \\ \xi(x,0) = \lambda_1'(x), \quad \xi(0,t) = \lambda_2'(t), \quad \xi(1,t) = \lambda_3'(t) \end{aligned} \quad (2)$$

In the concerned mathematical model (1)-(2), $\mu_1(x, t)$ and $\mu_2(x, t)$ denote the variable order derivatives which depend on space and time such that $g - 1 < \mu_1(x, t), \mu_2(x, t) < g$. Here g is the first integer not less than $\mu_1(x, t), \mu_2(x, t)$. The other terms $p_{i's}$ and $p'_{i's}$ denote some physical realistic constants, $h_1(x, t)$ and $h_2(x, t)$ are the source terms.

Here, our another aim is to develop a highly efficient and most powerful technique viz., the operational matrix method based on Bernstein polynomials to find the approximate numerical solution of the considered non-linear VO system of a coupled reaction-diffusion equation with given initial and boundary conditions.

Basic definitions and properties of Bernstein polynomials

Nowadays the Bernstein polynomials are world wide useful in different areas of engineering and applied mathematics [16, 17]. In the unit interval $[0, 1]$, Bernstein polynomials of degree l^{th} are defined:

$$B_{p,l}(x) = \binom{l}{p} x^p (1-x)^{l-p}, \quad 0 \leq p \leq l \quad (3)$$

As $0 \leq x \leq 1$, we can use binomial expansion in the aforementioned equation:

$$B_{p,l}(x) = \binom{l}{p} x^p \left[\sum_{s=0}^{l-p} (-1)^s \binom{l-p}{s} x^s \right], \quad 0 \leq p \leq l \quad (44)$$

or

$$B_{p,l}(x) = \sum_{s=0}^{l-p} (-1)^s \binom{l}{p} \binom{l-p}{s} x^{p+s}, \quad 0 \leq p \leq l \quad (5)$$

The Bernstein polynomials can be written in the matrix form:

$$\mathcal{G}(x) = MP_l(x) \quad (6)$$

where

$$\mathcal{G}(x) = [B_{0,l}(x), B_{1,l}(x), \dots, B_{l,l}(x)]^T \quad P_l(x) = [1, x, x^2, \dots, x^l]^T$$

and M is an upper triangular matrix given:

$$M = \begin{bmatrix} (-1)^0 \binom{l}{0} & (-1)^1 \binom{l}{0} \binom{l-0}{1-0} & \dots & \dots & \dots & (-1)^{m-0} \binom{l}{0} \binom{l-0}{1-0} \\ 0 & (-1)^0 \binom{l}{1} & \dots & \dots & \dots & (-1)^{m-1} \binom{l}{1} \binom{l-1}{l-1} \\ \vdots & \vdots & \vdots & \vdots & \vdots & \vdots \\ 0 & 0 & \dots & (-1)^0 \binom{l}{i} & \dots & (-1)^{m-i} \binom{l}{i} \binom{l-i}{l-i} \\ \vdots & \vdots & \vdots & \vdots & \vdots & \vdots \\ 0 & 0 & \dots & \dots & \dots & (-1)^0 \binom{l}{l} \end{bmatrix} \quad (7)$$

The format of matrix M reveals that it is an invertible matrix *i.e.*, $|M| \neq 0$. Few properties of Bernstein polynomials are given:

$$B_{p,l}(x) \geq 0, \quad \forall x \in [0,1]$$

i.e., Bernstein polynomials are always positive in their domain

$$B_{p,l}(1-x) = B_{l-p,l}(x)$$

and

$$B'_{p,l}(x) = l[B_{p-1,l-1}(x) - B_{p,l-1}(x)]$$

Approximations of the unknown functions $\zeta(x, t)$ and $\xi(x, t)$

Since the set of Bernstein polynomials forms a complete basis in the Hilbert space $L^2[0, 1]$ therefore, each function $\zeta(x) \in L^2[0, 1]$ can be expressed in terms of Bernstein polynomials:

$$\zeta(x) \simeq \zeta_r(x) = \sum_{g=0}^r b_g B_{g,r}(x) = B^T \mathcal{G}(x) \quad (8)$$

where $B^T = [b_g]$ is the unknown constant matrix, which is known as Bernstein coefficients.

Similarly, functions of two variables:

$$\zeta(x, t), \xi(x, t) \in L^2[0,1]$$

can be expanded in terms of Bernstein polynomials:

$$\begin{aligned} \zeta(x, t) \simeq \zeta_r(x, t) &= \sum_{g=0}^r \sum_{h=0}^r b_{g,h} B_{g,r}(x) B_{h,r}(t) = \mathcal{G}(x)^T B \mathcal{G}(t) \\ \xi(x, t) \simeq \xi_r(x, t) &= \sum_{g=0}^r \sum_{h=0}^r b'_{i,j} B_{i,r}(x) B_{j,r}(t) = \mathcal{G}(x)^T B' \mathcal{G}(t) \end{aligned} \quad (9)$$

where the unknown constant matrices $B = [b_{g,h}]$ and $B' = [b'_{ij}]$ are known as Bernstein coefficients. The initial and boundary conditions can be used to determine these coefficients.

Operational matrix of the variable order derivative

In this section of the manuscript, the operational matrix for the VO derivative is derived. With the help of eq. (6), the derivative of the vector $\mathcal{G}(t)$ can be written:

$$\frac{\partial^{\mu(x,t)} \mathcal{G}(t)}{\partial t^{\mu(x,t)}} = \frac{\partial^{\mu(x,t)} M P_r(t)}{\partial t^{\mu(x,t)}} = M \frac{\partial^{\mu(x,t)}}{\partial t^{\mu(x,t)}} \begin{bmatrix} 1 \\ t \\ t^2 \\ \vdots \\ t^{g-1} \\ t^g \\ \vdots \\ t^r \end{bmatrix} =$$

→

$$= M \begin{bmatrix} 0 & 0 & 0 & \dots & 0 & 0 & \dots & 0 & 0 \\ 0 & 0 & 0 & \dots & 0 & 0 & \dots & 0 & 0 \\ 0 & 0 & 0 & \dots & 0 & 0 & \dots & 0 & 0 \\ \vdots & \vdots & \vdots & \vdots & \vdots & \vdots & \vdots & \vdots & \vdots \\ 0 & 0 & 0 & \dots & 0 & 0 & \dots & 0 & 0 \\ 0 & 0 & 0 & \dots & 0 & \frac{\Gamma(g+1)t^{-\mu(x,t)}}{\Gamma[g+1-\mu(x,t)]} & \dots & 0 & 0 \\ \vdots & \vdots & \vdots & \vdots & \vdots & \vdots & \vdots & \vdots & \vdots \\ 0 & 0 & 0 & \dots & 0 & 0 & \dots & 0 & \frac{\Gamma(r+1)t^{-\mu(x,t)}}{\Gamma[r+1-\mu(x,t)]} \end{bmatrix} \begin{bmatrix} 1 \\ t \\ t^2 \\ \vdots \\ t^{g-1} \\ t^g \\ \vdots \\ t^r \end{bmatrix} \quad (10)$$

where $g - 1 \leq \mu(x, t) \leq g$, we take $g = [\mu(x, t)]$ and $g < r$.

From the aforementioned equation we can write:

$$\frac{\partial^{\mu(x,t)} \vartheta(t)}{\partial t^{\mu(x,t)}} = M \Omega P_r(t) = M \Omega M^{-1} \vartheta(t) \quad (11)$$

where Ω is given by the expression:

$$\Omega = [a_{pq}]_{(r+1) \times (r+1)} = \begin{cases} 0, & \text{elsewhere} \\ \frac{\Gamma(g+1)t^{-\mu(x,t)}}{\Gamma(g+1-\mu(x,t))}, & \text{when } p = q \geq g \end{cases} \quad (12)$$

where $M \Omega M^{-1}$ is an operational matrix w.r.t. time. The operational matrix for VO derivatives w.r.t. x can be obtained in a similar manner. Now, by collocating our considered model (1), and initial and boundary conditions (2), we get a system of non-linear algebraic equations which help to find the arbitrary constant matrices B and B' given in eq. (9).

Convergence analysis of the scheme

Theorem: Let the functions

$$\zeta(x, t), \xi(x, t) : [0, 1] \times [0, 1] \rightarrow \mathbb{R} \text{ are } (r+1)$$

times continuously differentiable functions, i.e.,

$$\zeta, \xi \in C^{r+1}[0, 1]^2, \text{ and let } \mathbb{X} = \text{Span}[B_{p,r}(x)B_{q,r}(t), p, q = 0, 1, \dots, r]$$

is a vector space. Let:

$$\vartheta(x)^T B \vartheta(t) \text{ and } \vartheta(x)^T B' \vartheta(t)$$

are best approximations of the functions $\zeta(x, t)$ and $\xi(x, t)$, respectively out of \mathbb{X} , then the mean error bounds are given:

$$\begin{aligned} \|\zeta(x, t) - \vartheta(x)^T B \vartheta(t)\|_2 &\leq \frac{\sqrt{sc}}{(r+1)!} \frac{r+2}{2^{2r+4}} \\ \|\xi(x, t) - \vartheta(x)^T B' \vartheta(t)\|_2 &\leq \frac{\sqrt{s'c}}{(r+1)!} \frac{r+2}{2^{2r+4}} \end{aligned} \quad (13)$$

where error bounds

$$s = \max[s_0, s_1, \dots, s_{r+1}], \quad s' = \max[s'_0, s'_1, \dots, s'_{r+1}], \quad \text{and} \quad c = \max\left[\binom{r+1}{a}, 0 \leq a \leq r+1\right]$$

Proof: The Taylor series approximation of the function $\zeta(x, t)$ in the neighborhood of a point (x_0, t_0) is given:

$$\zeta_r(x, t) = \zeta(x_0, t_0) + \zeta'_x(x_0, t_0)(x - x_0) + \zeta'_t(x_0, t_0)(t - t_0) + \dots \quad (14)$$

from which we can obtain

$$|\zeta(x, t) - \zeta_r(x, t)| = \left| \frac{1}{(r+1)!} \sum_{a=0}^{r+1} \binom{r+1}{a} \zeta_{x^{r+1-a}t^a}(x_0, t_0) (x - x_0)^{r+1-a} (t - t_0)^a \right| \quad (15)$$

Suppose that $\mathcal{G}(x)^T B \mathcal{G}(t)$ be the best approximation of $\zeta(x, t)$, then:

$$\|\zeta(x, t) - \mathcal{G}(x)^T B \mathcal{G}(t)\|_2^2 \leq \|\zeta(x, t) - \zeta_r(x, t)\|_2^2 = \int_0^1 \int_0^1 |\zeta(x, t) - \zeta_r(x, t)|^2 dx dt \quad (16)$$

In view of eq. (15), we have:

$$\begin{aligned} \|\zeta(x, t) - \mathcal{G}(x)^T B \mathcal{G}(t)\|_2^2 &\leq \int_0^1 \int_0^1 \left| \frac{1}{(r+1)!} \sum_{a=0}^{r+1} \binom{r+1}{a} \zeta_{x^{r+1-a}t^a}(x_0, t_0) \cdot \right. \\ &\quad \left. \cdot (x - x_0)^{r+1-a} (t - t_0)^a \right|^2 dx dt \end{aligned} \quad (17)$$

It is assumed that

$$\zeta_{x^{r+1-a}t^a}(x, t)$$

is $(r+1)$ times continuously differentiable function, therefore, there exist constants s_0, s_1, \dots, s_{r+1} :

$$\max_{0 \leq x, t \leq 1} \zeta_{x^{r+1-a}t^a}(x, t) \leq s_a, \quad 0 \leq a \leq r+1 \quad (18)$$

Now we have:

$$\|\zeta(x, t) - \mathcal{G}(x)^T B \mathcal{G}(t)\|_2^2 \leq \int_0^1 \int_0^1 \left| \frac{1}{(r+1)!} \sum_{a=0}^{r+1} \binom{r+1}{a} s_a (x - x_0)^{r+1-a} (t - t_0)^a \right|^2 dx dt \quad (19)$$

Considering

$$s = \max[s_0, s_1, \dots, s_{r+1}] \quad \text{and} \quad c = \max\left[\binom{r+1}{a}, 0 \leq a \leq r+1\right]$$

the eq. (19) becomes:

$$\|\zeta(x, t) - \mathcal{G}(x)^T B \mathcal{G}(t)\|_2^2 \leq \frac{sc}{(r+1)!^2} \int_0^1 \int_0^1 \left| \sum_{a=0}^{r+1} (x - x_0)^{r+1-a} (t - t_0)^a \right|^2 dx dt \quad (20)$$

Suppose that y_j be the roots of Bernstein Polynomials. For the term $(x - x_0)^{r+1-a}$, one can find the following bounds by using the mapping $x = (y + 1)/2$ between the intervals $[-1, 1]$ and $[0, 1]$:

$$\min_{0 \leq x_j \leq 1} \max_{0 \leq x \leq 1} |(x - x_0)^{r+1-a}| = \min_{0 \leq y_j \leq 1} \max_{0 \leq y \leq 1} \left| \left(\frac{y - y_j}{2} \right)^{r+1-a} \right| = \frac{1}{2^{2(r+1-a)+1}} \quad (21)$$

Thus from the equation (20), we can write:

$$\left\| \zeta(x, t) - \mathcal{G}(x)^T B \mathcal{G}(t) \right\|_2^2 \leq \frac{sc}{(r+1)!^2} \int_0^1 \int_0^1 \left| \sum_{a=0}^{r+1} \frac{1}{2^{2(r+1-a)+1}} \frac{1}{2^{2a+1}} \right|^2 dx dt \quad (22)$$

or

$$\left\| \zeta(x, t) - \mathcal{G}(x)^T B \mathcal{G}(t) \right\|_2^2 \leq \frac{sc}{(r+1)!^2} \frac{(r+2)^2}{2^{4r+8}} \quad (23)$$

Now taking the square root on both sides of previous equation, we get our desired error bound. Similarly, the error bound for $\xi(x, t)$ can be calculated.

Numerical simulations and error analysis

In this section, the operational matrix method based on Bernstein polynomials has been applied to some non-linear VO coupled PDE to show the accuracy and efficiency of the presented numerical technique through error analysis. The software MATHEMATICA 11.3 is used for the whole numerical computation. The amount of time taken by the program code for numerical outputs in MATHEMATICA 11.3 increases slowly as the order of approximation r is increased, *i.e.*, time complexity increases with the increase in order of approximation.

Example 1. Coupled Whitham-Broer-Kaup (WBK) equations: consider the non-linear coupled reaction-diffusion equations with variable order:

$$\begin{aligned} \frac{\partial^{\mu_1(x,t)} \zeta(x,t)}{\partial t^{\mu_1(x,t)}} + \frac{\partial^2 \zeta(x,t)}{\partial x^2} + \frac{\partial \xi(x,t)}{\partial x} + \zeta(x,t) \frac{\partial \zeta(x,t)}{\partial x} &= h_1(x,t) \\ \frac{\partial^{\mu_2(x,t)} \xi(x,t)}{\partial t^{\mu_2(x,t)}} + \frac{\partial^3 \zeta(x,t)}{\partial x^3} - \frac{\partial^3 \xi(x,t)}{\partial x^3} + \frac{\partial(\zeta(x,t)\xi(x,t))}{\partial x} &= h_2(x,t) \end{aligned} \quad (24)$$

This system of PDE explains many physical phenomena arising in fluid mechanics. This equation is known as system of coupled WBK equations. The analytical solutions of this coupled system are

$$\zeta(x,t) = \frac{4}{1 + \exp(2(x-3t))} \quad \text{and} \quad \xi(x,t) = \frac{3 \exp[2(x-3t)]}{\{1 + \exp[2(x-3t)]\}^2}$$

with suitable values of $h_1(x, t)$ and $h_2(x, t)$. The initial and boundary conditions can be derived from the exact solution of the problem. The L_2 norm error and L_∞ normed errors between the exact solutions and the solutions obtained by our proposed method are shown through tabs. 1 and 2 for different values of fractional orders $\mu_1(x, t)$ and $\mu_2(x, t)$, respectively at different values of time, t , and for different order of approximation r . We can easily find the fact that these errors decrease as the order of approximation increases. This error analysis shows the high efficiency of the proposed numerical scheme during the computation of numerical solution. Hence comparing the numerical solution and exact solution, one can ensure the effectiveness and efficiency of this numerical scheme.

Table 1. Comparison of L_∞ and L_2 norm errors for $\zeta(x, t)$ at $t = 0.05$

r	$\mu_1(x, t) = \frac{e^{-t} \cos x}{400}$		$\mu_1(x, t) = \frac{2 \cos x + \sin t}{400}$		$\mu_1(x, t) = \frac{\sin t + e^{-t} \cos x}{300}$	
	L_∞	L_2	L_∞	L_2	L_∞	L_2
4	$5.23 \cdot 10^{-10}$	$5.42 \cdot 10^{-10}$	$5.98 \cdot 10^{-10}$	$6.04 \cdot 10^{-10}$	$6.24 \cdot 10^{-10}$	$6.43 \cdot 10^{-10}$
5	$6.73 \cdot 10^{-12}$	$6.92 \cdot 10^{-12}$	$2.29 \cdot 10^{-12}$	$5.53 \cdot 10^{-11}$	$3.67 \cdot 10^{-11}$	$6.83 \cdot 10^{-11}$
6	$4.20 \cdot 10^{-13}$	$8.83 \cdot 10^{-13}$	$3.18 \cdot 10^{-13}$	$7.64 \cdot 10^{-13}$	$7.46 \cdot 10^{-13}$	$8.37 \cdot 10^{-12}$
7	$1.09 \cdot 10^{-16}$	$5.64 \cdot 10^{-15}$	$2.78 \cdot 10^{-16}$	$4.00 \cdot 10^{-16}$	$4.64 \cdot 10^{-16}$	$1.02 \cdot 10^{-15}$

Table 2. Comparison of L_∞ and L_2 norm errors for $\zeta(x, t)$ at $t = 0.05$

r	$\mu_2(x, t) = \frac{e^{-t} \cos x}{400}$		$\mu_2(x, t) = \frac{2 \cos x + \sin t}{400}$		$\mu_2(x, t) = \frac{\sin t + e^{-t} \cos x}{300}$	
	L_∞	L_2	L_∞	L_2	L_∞	L_2
4	$5.34 \cdot 10^{-10}$	$8.23 \cdot 10^{-10}$	$4.24 \cdot 10^{-10}$	$5.30 \cdot 10^{-10}$	$9.94 \cdot 10^{-10}$	$3.03 \cdot 10^{-09}$
5	$1.39 \cdot 10^{-12}$	$4.54 \cdot 10^{-12}$	$4.39 \cdot 10^{-12}$	$5.84 \cdot 10^{-12}$	$6.43 \cdot 10^{-12}$	$5.34 \cdot 10^{-11}$
6	$4.34 \cdot 10^{-14}$	$1.09 \cdot 10^{-13}$	$1.54 \cdot 10^{-13}$	$4.63 \cdot 10^{-13}$	$2.12 \cdot 10^{-13}$	$4.03 \cdot 10^{-13}$
7	$6.33 \cdot 10^{-16}$	$7.40 \cdot 10^{-16}$	$3.53 \cdot 10^{-16}$	$1.43 \cdot 10^{-15}$	$1.64 \cdot 10^{-16}$	$5.32 \cdot 10^{-16}$

Example 2. Coupled KdV-Burgers equations: Consider a particular case of the model (1), which is the following non-linear VO coupled reaction-diffusion equations:

$$\begin{aligned} \frac{\partial^{\mu_1(x,t)} \zeta(x,t)}{\partial t^{\mu_1(x,t)}} + \frac{\partial^3 \zeta(x,t)}{\partial x^3} + \frac{\partial^2 \xi(x,t)}{\partial x^2} + \zeta(x,t) \frac{\partial \zeta(x,t)}{\partial x} &= h_1(x,t) \\ \frac{\partial^{\mu_2(x,t)} \xi(x,t)}{\partial t^{\mu_2(x,t)}} + \frac{\partial^3 \zeta(x,t)}{\partial x^3} + \frac{\partial^2 \xi(x,t)}{\partial x^2} + \xi(x,t) \frac{\partial \xi(x,t)}{\partial x} &= h_2(x,t) \end{aligned} \tag{25}$$

This system of coupled PDE describes several physical phenomena arising in non-linear optics and non-linear wave theory. This system is known as system of coupled KdV-Burgers equations. The analytical solutions of this coupled system are

$$\zeta(x, t) = \exp(x+t) \sin(xt) \quad \text{and} \quad \xi(x, t) = \exp(x+t) \cos(xt)$$

with suitable values of $h_1(x, t)$ and $h_2(x, t)$. The error analysis through the comparison of L_2 and L_∞ is shown through the tabs. 3 and 4 for different values of fractional order $\mu_1(x, t)$ and $\mu_2(x, t)$, respectively and for various values of t and r . We can easily find the fact that these errors decrease as the order of approximation increases. This error analysis shows the high efficiency and accuracy of proposed numerical scheme during the computation of numerical solution.

Table 3. Comparison of L_∞ and L_2 norm errors for $\zeta(x, t)$ at $t = 0.05$

r	$\mu_1(x, t) = \frac{\cos t + e^{-2t} \sin x}{300}$		$\mu_1(x, t) = \frac{e^{-2t} \sin x}{400}$		$\mu_1(x, t) = \frac{\sin t + e^{-t} \cos x}{400}$	
	L_∞	L_2	L_∞	L_2	L_∞	L_2
4	$1.06 \cdot 10^{-10}$	$2.13 \cdot 10^{-10}$	$2.74 \cdot 10^{-10}$	$7.75 \cdot 10^{-10}$	$6.86 \cdot 10^{-10}$	$8.63 \cdot 10^{-10}$
5	$3.76 \cdot 10^{-11}$	$4.86 \cdot 10^{-11}$	$4.86 \cdot 10^{-11}$	$5.84 \cdot 10^{-11}$	$1.53 \cdot 10^{-11}$	$5.95 \cdot 10^{-11}$
6	$7.54 \cdot 10^{-13}$	$8.26 \cdot 10^{-13}$	$5.85 \cdot 10^{-13}$	$7.28 \cdot 10^{-12}$	$5.86 \cdot 10^{-13}$	$7.73 \cdot 10^{-13}$
7	$9.86 \cdot 10^{-15}$	$9.94 \cdot 10^{-15}$	$2.96 \cdot 10^{-15}$	$4.86 \cdot 10^{-15}$	$1.56 \cdot 10^{-15}$	$8.86 \cdot 10^{-14}$

Table 4. Comparison of L_∞ and L_2 norm errors for $\zeta(x, t)$ at $t = 0.05$

r	$\mu_2(x, t) = \frac{\cos t + e^{-2t} \sin x}{300}$		$\mu_2(x, t) = \frac{e^{-2t} \sin x}{400}$		$\mu_2(x, t) = \frac{\sin t + e^{-t} \cos x}{400}$	
	L_∞	L_2	L_∞	L_2	L_∞	L_2
4	$7.93 \cdot 10^{-10}$	$7.98 \cdot 10^{-10}$	$4.32 \cdot 10^{-10}$	$6.42 \cdot 10^{-10}$	$1.02 \cdot 10^{-10}$	$1.64 \cdot 10^{-10}$
5	$6.41 \cdot 10^{-11}$	$4.32 \cdot 10^{-10}$	$4.22 \cdot 10^{-11}$	$8.94 \cdot 10^{-11}$	$6.42 \cdot 10^{-11}$	$8.43 \cdot 10^{-11}$
6	$4.32 \cdot 10^{-13}$	$6.34 \cdot 10^{-12}$	$8.53 \cdot 10^{-13}$	$9.64 \cdot 10^{-13}$	$5.75 \cdot 10^{-13}$	$7.33 \cdot 10^{-13}$
7	$6.48 \cdot 10^{-15}$	$3.42 \cdot 10^{-14}$	$6.34 \cdot 10^{-15}$	$7.53 \cdot 10^{-15}$	$1.53 \cdot 10^{-15}$	$6.34 \cdot 10^{-15}$

Example 3. Coupled Burgers equation: here a particular case of the model (1) is considered:

$$\begin{aligned} \frac{\partial^{\mu_1(x,t)} \zeta(x,t)}{\partial t^{\mu_1(x,t)}} - \frac{\partial^2 \zeta(x,t)}{\partial x^2} - 2\zeta(x,t) \frac{\partial \zeta(x,t)}{\partial x} + \frac{\partial [\zeta(x,t)\xi(x,t)]}{\partial x} &= h_1(x,t) \\ \frac{\partial^{\mu_2(x,t)} \zeta(x,t)}{\partial t^{\mu_2(x,t)}} - \frac{\partial^2 \xi(x,t)}{\partial x^2} - 2\xi(x,t) \frac{\partial \xi(x,t)}{\partial x} + \frac{\partial [\zeta(x,t)\xi(x,t)]}{\partial x} &= h_2(x,t) \end{aligned} \tag{26}$$

This system of coupled PDE has wide range of applications in several physical phenomena like fluid mechanics, gas dynamics, non-linear acoustics. This equation is known as system of coupled Burgers equation. The analytical solutions of this coupled system are:

$$\zeta(x, t) = e^{-t} \sin x \text{ and } \xi(x, t) = e^{-t} \sin x$$

with suitable values of $h_1(x, t)$ and $h_2(x, t)$. The error analysis through the comparison of L_2 and L_∞ is shown through tabs. 5 and 6 for different values of $\mu_1(x, t)$ and $\mu_2(x, t)$, respectively, and for different values of t and r . It is seen that the errors decrease as the order of approximation increases. This error analysis shows the high efficiency of the proposed numerical scheme during the computation of numerical solution.

Table 5. Comparison of L_∞ and L_2 norm errors for $\zeta(x, t)$ at $t = 0.05$

r	$\mu_1(x, t) = \frac{2 \cos t + e^{-2t} \sin 2x}{300}$		$\mu_1(x, t) = \frac{2e^{-2t} \cos x}{400}$		$\mu_1(x, t) = \frac{\sin 2t + 2e^{-t} \cos x}{400}$	
	L_∞	L_2	L_∞	L_2	L_∞	L_2
4	$9.02 \cdot 10^{-10}$	$1.83 \cdot 10^{-09}$	$2.56 \cdot 10^{-10}$	$4.38 \cdot 10^{-10}$	$1.17 \cdot 10^{-10}$	$4.27 \cdot 10^{-10}$
5	$5.26 \cdot 10^{-11}$	$8.51 \cdot 10^{-11}$	$1.03 \cdot 10^{-11}$	$4.32 \cdot 10^{-11}$	$2.14 \cdot 10^{-11}$	$4.63 \cdot 10^{-11}$
6	$1.86 \cdot 10^{-13}$	$3.94 \cdot 10^{-13}$	$7.54 \cdot 10^{-14}$	$1.76 \cdot 10^{-13}$	$6.86 \cdot 10^{-13}$	$5.43 \cdot 10^{-12}$
7	$5.34 \cdot 10^{-16}$	$6.45 \cdot 10^{-16}$	$5.04 \cdot 10^{-16}$	$3.85 \cdot 10^{-15}$	$7.54 \cdot 10^{-16}$	$9.54 \cdot 10^{-15}$

Table 6. Comparison of L_∞ and L_2 norm errors for $\zeta(x, t)$ at $t = 0.05$

r	$\mu_2(x, t) = \frac{2 \cos t + e^{-2t} \sin 2x}{300}$		$\mu_2(x, t) = \frac{2e^{-2t} \cos x}{400}$		$\mu_2(x, t) = \frac{\sin 2t + 2e^{-t} \cos x}{400}$	
	L_∞	L_2	L_∞	L_2	L_∞	L_2
4	$1.75 \cdot 10^{-10}$	$7.58 \cdot 10^{-10}$	$1.65 \cdot 10^{-10}$	$8.56 \cdot 10^{-10}$	$8.98 \cdot 10^{-10}$	$9.48 \cdot 10^{-10}$
5	$4.42 \cdot 10^{-12}$	$1.49 \cdot 10^{-11}$	$4.04 \cdot 10^{-12}$	$9.70 \cdot 10^{-11}$	$6.43 \cdot 10^{-11}$	$9.73 \cdot 10^{-11}$
6	$7.95 \cdot 10^{-13}$	$1.03 \cdot 10^{-13}$	$7.53 \cdot 10^{-13}$	$8.09 \cdot 10^{-13}$	$5.81 \cdot 10^{-13}$	$8.41 \cdot 10^{-12}$
7	$5.73 \cdot 10^{-15}$	$6.75 \cdot 10^{-15}$	$3.90 \cdot 10^{-15}$	$1.86 \cdot 10^{-14}$	$1.62 \cdot 10^{-15}$	$9.76 \cdot 10^{-15}$

Results and discussion

After the validation of the efficiency of the proposed numerical method through applying it on three given examples in the previous section, the authors have made an endeavour to apply it in the considered mathematical models (1) and (2) for different particular values of the parameters. The behaviors of solute concentration for different variable order are shown in the following figures for different values of constant coefficients.

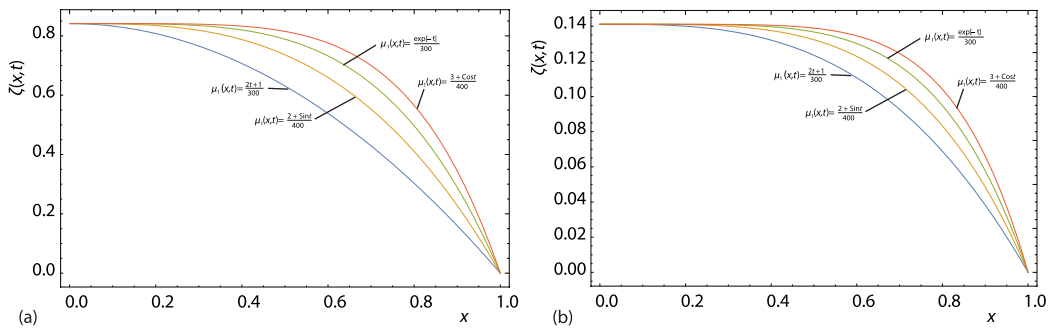


Figure 1. Plots of $\zeta(x, t)$ vs. x for different fractional variable order for (a) $p_1 = -1$ and (b) $p_1 = 1$

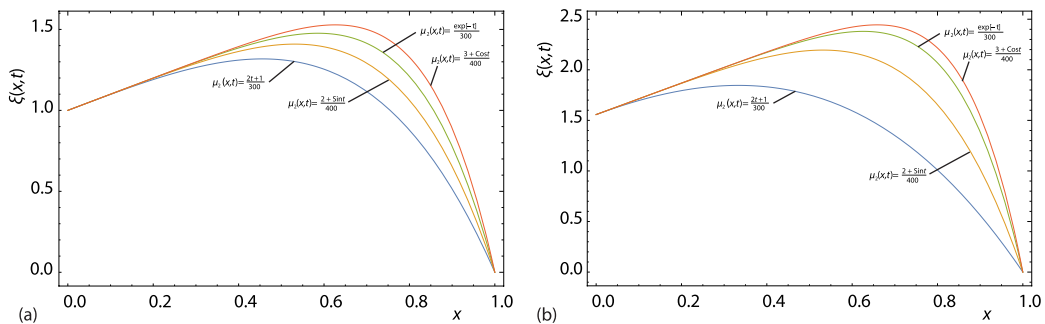


Figure 2. Plots of $\zeta(x, t)$ vs. x for different fractional variable order for (a) $p'_3 = 1$ and (b) $p'_3 = -1$

The overshoots of solute profiles $\zeta(x, t)$ and $\zeta(x, t)$ for different variable orders $\mu_1(x, t)$ and $\mu_2(x, t)$ at $t = 1$ are shown through the figs. 1 and 2. Figures 1(a) and 1(b) are the plots of solute profile $\zeta(x, t)$ vs. spatial variable x for $p_1 = 1$ and $p_1 = -1$, respectively, when other constant coefficients are taken as

$$p_2 = 1.2 = p_4 = p'_2 = p'_4, \quad p_3 = 1 = p_5 = p_6 = p'_1 = p'_3 = p'_5 = p'_6$$

Figures 2(a) and 2(b) are the plots of solute profile $\zeta(x, t)$ vs. spatial variable x for $p'_3 = 1$ and $p'_3 = -1$, respectively when other constant coefficients are taken as

$$p_2 = 1.2 = p_4 = p'_2 = p'_4, \quad p_1 = 1 = p_3 = p_5 = p_6 = p'_1 = p'_5 = p'_6$$

The effects of advection term are also justified from variations of the solute profile as shown in the said figures.

Conclusions

Present research manuscript provides three useful consequences, are as follows.

- The derivation of Bernstein operational matrices of VO derivatives w.r.t. time and space.

- The proper utilisation of the collocation technique with the Bernstein polynomials to solve the non-linear VO coupled system of a reaction-diffusion equation with the prescribed initial and boundary conditions.
- Finding the error bounds and stability analysis for the approximation and demonstration of error analysis. Overshoots of solute concentration have also been justified in the article. The authors are optimistic that in future, their proposed efficient technique can be applied to solve more complex physical models like 2-D non-linear VO reaction-advection-diffusion and the 2-D VO coupled system of equations.

References

- [1] Mirzaee, F., Hoseini, S. F., Hybrid Functions of Bernstein Polynomials and Blockpulse Functions for Solving Optimal Control of the Non-linear Volterra Integral Equations, *Indagationes Mathematicae*, 27 (2016), 3, pp. 835-849
- [2] Mirzaee, F., Samadyar, N., Numerical Solution Based on 2-D Orthonormal Bernstein Polynomials for Solving Some Classes of 2-D Non-linear Integral Equations of Fractional Order, *Applied Mathematics and Computation*, 344 (2019), Mar., pp. 191-203
- [3] Das, S., Analytical Solution of a Fractional Diffusion Equation by Variational Iteration Method, *Computers and Mathematics with Applications*, 57 (2009), 3, pp. 483-487
- [4] Das, S., et al., Solution of the Non-Linear Fractional Diffusion Equation with Absorbent Term and External Force, *Applied Mathematical Modelling*, 35 (2011), 8, pp. 3970-3979
- [5] Mirzaee, F., Samadyar, N., Application of Orthonormal Bernstein Polynomials to Construct an Efficient Scheme for Solving Fractional Stochastic Integro-Differential Equation, *Optik*, 132 (2017), Mar., pp. 262-273
- [6] Arikoglu, A., Ozkol, I., Solution of Fractional Differential Equations by Using Differential Transform Method, *Chaos, Solitons and Fractals*, 34 (2007), 5, pp. 1473-1481
- [7] Das, S., Rajeev, Solution of Fractional Diffusion Equation with a Moving Boundary Condition by Variational Iteration Method and Adomian Decomposition Method, *Zeitschrift für Naturforschung A*, 65 (2010), 10, pp. 793-799
- [8] Pandey, P., et al., An Operational Matrix for Solving Time-Fractional Order Cahn-Hilliard Equation, *Thermal Science*, 23 (2019), Suppl. 6, pp. S2045-S2052
- [9] Pandey, P., et al., The 2-D Non-linear Time Fractional Reaction-Diffusion Equation in Application Sub-Diffusion Process of the Multicomponent Fluid in Porous Media, *Meccanica*, 56 (2021), 1, pp. 99-115
- [10] Ganji, R. M., Jafari, H., A Numerical Approach for Multi-Variable Orders Differential Equations Using Jacobi Polynomials, *International Journal of Applied and Computational Mathematics*, 5 (2019), 2, pp. 1-9
- [11] Valerio, D., Costa, J., Variable Order Fractional Controllers, *Asian Journal of Control*, 15 (2013), 3, pp. 648-657
- [12] Ortigueira, M. D., et al., Variable Order Fractional Systems, *Communications in Non-linear Science and Numerical Simulation*, 71 (2019), June, pp. 231-243
- [13] Fu, Z.-J., et al., Method of Approximate Particular Solutions for Constant and Variable-Order Fractional Diffusion Models, *Engineering Analysis with Boundary Elements*, 57 (2015), Aug., pp. 37-46
- [14] Chen, R., et al., Numerical Methods and Analysis for a Multi-Term Time-Space Variable-Order Fractional Advection-Diffusion Equations and Applications, *Journal of Computational and Applied Mathematics*, 352 (2019), May, pp. 437-452
- [15] Lin, R., et al., Stability and Convergence of a New Explicit Finite Difference Approximation for the Variable-Order Non-Linear Fractional Diffusion Equation, *Applied Mathematics and Computation*, 212 (2009), 2, pp. 435-445
- [16] Yousefi, S. A., Behroozifar, M., Operational Matrices of Bernstein Polynomials and Their Applications, *International Journal of Systems Science*, 41 (2010), 6, pp. 709-716
- [17] Chen, Y.-M., et al., Numerical Study of a Class of Variable Order Non-Linear Fractional Differential Equation in Terms of Bernstein Polynomials, *Ain Shams Engineering Journal*, 9 (2018), 4, pp. 1235-1241